20th-century climate change inferred from four long-term point observations of seasonal mass balance

Matthias HUSS, Andreas BAUDER

Laboratory of Hydraulics, Hydrology and Glaciology (VAW), ETH Zürich, 8092 Zürich, Switzerland
E-mail: huss@vaw.baug.ethz.ch

ABSTRACT. Four long-term time series of seasonal mass-balance observations, all starting in 1914, have been compiled for two stakes on Claridenfirn and one stake on Grosser Aletschgletscher and Silvrettagletscher, Switzerland. These data represent the longest records of mass balance worldwide. A mass-balance model based on the temperature-index approach is used to correct field data for varying observation dates and data gaps and to separate accumulation and ablation. The homogenized continuous 93 year time series cover most of the 20th century and enable us to investigate temporal, regional and altitudinal variability in mass balance and changes in the climatic forcing on glaciers. A high-altitude site shows summer balance trends opposite to those at three stakes located near the equilibrium line. Since 1975, melt rates have increased by 10% $(10\,a)^{-1}$ periods of enhanced climatic forcing are detected: 1943–53 and 1987–2007. The energy consumed for melt was higher in the 1940s despite lower air temperatures compared to the years since 1987. We find evidence for a change in the glacier surface heat budget, which has important implications for the long-term stability of degree-day factors in empirical temperature-index modelling.

INTRODUCTION

Changes in glacier surface mass balance are considered to be a sensitive indicator for climatic variations (e.g. Vincent and others, 2004; Kaser and others, 2006). Point observations at fixed locations directly reflect climatic conditions and are not biased by uncertain spatial interpolation of mass balance or the change in glacier surface area (Ohmura and others, 2007). Glacier surface mass balance in mid-latitudes is mainly determined by two processes: solid precipitation (accumulation) dominating the winter balance and snow- or ice melt (ablation) dominating the summer balance. Thus, seasonal mass-balance components most clearly reveal the effect of the climatic forcing on glaciers (Vincent and others, 2004). Accumulation on glaciers is generally regarded as the best measure for precipitation in high mountain regions.

The direct observation of seasonal mass balance is laborious and requires two field surveys: one in spring when the maximum of snow cover is reached, and one in late summer at the end of the melting season. In Switzerland, mass-balance measurements began in the 1910s on Claridenfirn, Grosser Aletschgletscher and Silvrettagletscher (Aellen, 1996). Seasonal observations at these locations were continued until today with almost no disruptions and represent the longest direct measurements of mass balance worldwide.

Müller and Kappenberger (1991) compiled the measurements at the two stakes on Claridenfirn and reconstructed missing data using regression methods. The Claridenfirn data have been repeatedly analyzed (Müller-Lemans and others, 1995; Vincent and others, 2004; Ohmura and others, 2007) and were discovered to be of great value for inferring climatic fluctuations at high altitudes in the Alps in the 20th century. The two comparable time series of Silvrettagletscher and Aletschgletscher, however, have not yet been considered in scientific discussions. In this study, we present four 93 year time series of seasonal point-based mass balance. The series are homogenized using a mass-balance model based on the temperature-index approach and now cover annual time periods of equal length. Accumulation and ablation components are separated, enabling the calculation of the total energy consumed for melt. We aim to analyze trends and regional differences in the context of 20th-century climatic forcing on Alpine glaciers. Changes in the heat budget at four high-alpine sites are investigated and the long-term stability of degree-day factors in empirical temperature-index modelling is assessed.

STUDY SITES AND FIELD DATA

With the aim of improved understanding of the precipitation conditions in high mountains, snow accumulation and mass-balance observations began at two sites on Claridenfirn in 1914 and 1915, at one site on Silvrettagletscher in 1915 and on Aletschgletscher in 1918 (Fig. 1). All series have continued until today (Table 1). The measurement sites are located at or above the long-term equilibrium line in locally flat terrain. Grosser Aletschgletscher is the largest ice mass in the Alps and borders the main northern Alpine crest. Claridenfirn and Silvrettagletscher are smaller mountain glaciers situated at the northern flank of the Swiss Alps.

The monitoring programme was consistent at all sites (Firnberichte, 1914–78; Glaciological reports, 1916–2008). The winter field survey is generally performed between April and June and the sites are visited again in September. Readings of the snow depth are complemented by density information; however, this was not systematically reported before 1960. Snow depth is evaluated using three independent methods: (1) differences in snow depth from readings at the stake; (2) snow probings; and (3) observations in snow pits or by drillings to a marked horizon including snow density measurements. Results from more than one of these procedures are often documented.

The stake marks the measurement site and is annually moved back to the initial position. The datasets are not complete (Fig. 2); stakes were lost due to high accumulation,
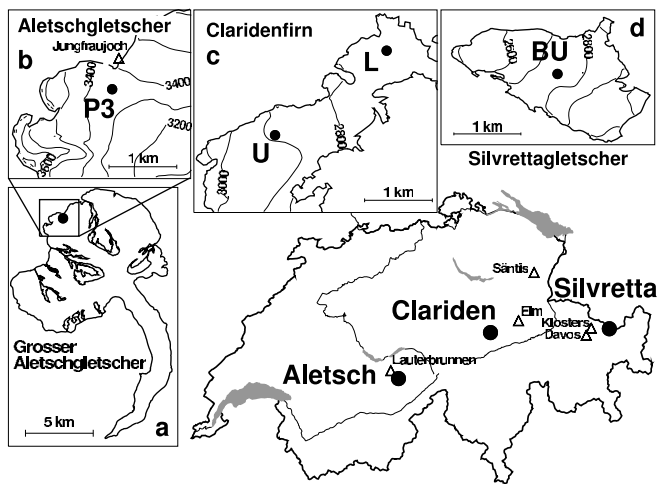
Fig. 1. Location of the study sites in Switzerland. Weather stations of MeteoSchweiz used in this study are indicated with triangles (Table 1). The local topographic setting of each stake is shown in insets (a–d). The contour interval is 100 m.
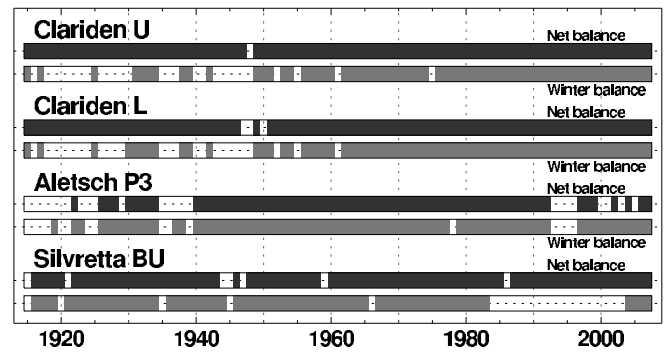

Fig. 2. Seasonal observations of point-based net and winter balance since 1914. The bars are unshaded for years with missing data.

METHODS

Time-series homogenization

In order to compare the time series, homogenization of the measurements is required to account for inconsistency, systematic errors and gaps in the reported observations (Fig. 2). The measurements were taken at arbitrary dates. Year-to-year differences of several months in the dates of field surveys have a considerable impact on the representativeness of the seasonal mass-balance results (Huss and others, 2008b). By applying a mass-balance model at a daily timescale, the observations are projected to common periods with fixed dates. Net balance b_n (m w.e.) is determined in the hydrological year (1 October–30 September). We subdivided the year into a winter (1 October–30 April) and summer period (1 May–September) for determination of winter and summer balance, b_w and b_s, respectively. We term mass-balance quantities at a single point as 'specific' mass balance (Meier, 1962). The model further allows us to handle incomplete years, to close gaps in a consistent way and to separate the total annual accumulation c_a from the total annual ablation a_a. In the homogenization procedure, measured weather data are used to resolve the seasonal mass-balance measurements on a daily scale.

Mass-balance model

We calculate daily specific mass balance using a temperature-index melt and accumulation model (Hock, 1999). Temperature-index models are based on a linear relation between melt rate and positive air temperature (Ohmura, 2001). In our approach, the degree-day factors are varied as a function of potential direct solar radiation in order to account for the effects of slope, aspect and shading (Hock,

and in a few cases a whole campaign did not take place. The location of stake Silvretta BU was moved about 200 m to the north in 1987 with no significant change in elevation. Until 1984, the data for the stakes Clariden U and L are taken from Müller and Kappenberger (1991). We discarded reconstructed data points for our analysis. The mass-balance data of Aletsch P3 and Silvretta BU are digitized from annual reports (Firnberichte, 1914–78; Glaciological reports, 1916–2008).

We also make use of topographical information and weather data (Table 1). For each of the three investigated glaciers, between four and eight digital elevation models (DEMs) exist covering the last century (Bauder and others, 2007). This allows the surface elevation change at the stake sites to be inferred. From the network of the official Swiss weather service (MeteoSchweiz) we use time series of daily air temperature recorded at Säntis (2490 m a.s.l., 54 km from Clariden), Jungfraujoch (3580 m a.s.l., 500 m from the stake site) and Davos (1590 m a.s.l., 18 km from Silvretta). The temperature records of Säntis and Davos have been corrected for biases due to changing measurement techniques or station relocation (Begert and others, 2005). Time series of daily precipitation are taken from Elm (965 m a.s.l., 21 km from Clariden), Lauterbrunnen (820 m a.s.l., 8 km from Aletsch), Davos and, since 1961, Klosters (1200 m a.s.l., 13 km from Silvretta) (Fig. 1).

Table 1. Measurement sites and data characteristics (elevation in m a.s.l. of stakes corresponds to the year 2003; number of missing winter and net balance observations refers to the entire study period 1914–2007)

Stake	Glacier	Elevation	Period	Missing balance values		Weather stations		Data source
				Net	Winter	Temperature	Precipitation	
U	Claridenfirn	2894	1915–2007	1	28	Säntis	Elm	*†‡
L	Claridenfirn	2679	1914–2007	3	27	Säntis	Elm	*†‡
P3	Gr. Aletschgletscher	3338	1918–2007	24	16	Jungfraujoch	Lauterbrunnen	*†
BU	Silvrettagletscher	2732	1915–2007	7	25	Davos	Davos, Klosters	*†

*Firnberichte (1914–78). †Glaciological reports (1916–2008). ‡Müller and Kappenberger (1991).

1999). Daily temperature and precipitation are required as input data. Surface melt rates M (m d^{-1}) at the stake site are calculated as

$$M = \begin{cases} \left(F_M + r_{snow/firn}\, I\right) T & T > 0 \\ 0 & T \leq 0, \end{cases} \tag{1}$$

where F_M (m d^{-1} °C^{-1}) denotes a melt factor, $r_{snow/firn}$ (m^3 W^{-1} d^{-1} °C^{-1}) are radiation factors for snow and firn surfaces and I (W m^{-2}) is the potential direct radiation.

Air temperature T (°C) at the stake is calculated using constant monthly temperature lapse rates determined by comparing several nearby weather stations. Annually updated surface elevation of the sites is obtained by linearly interpolating between two successive DEMs. The lapse rates vary between –4°C km^{-1} (January) and –6.5°C km^{-1} (June). Accumulation is computed using the daily precipitation sums at the weather station multiplied by a correction factor C_{prec}. A threshold temperature of 1.5°C distinguishes snow from rainfall. Using calculated melt and accumulation, the snow water equivalent S (m w.e.) at the stake site is updated daily. Ablation due to sublimation can occur on Alpine glaciers (Lang and others, 1977), but is of minor importance compared to melt. Sublimation is not included explicitly in the model. However, it is captured by the in situ mass-balance measurements.

Model calibration

The model calibration is an automated iterative procedure that is repeated for every year of the study period. The calculated mass balance is matched with the two annual direct observations (b_w, b_n) aiming at an exact fit. In order to avoid an underdetermined system, the free parameters of the mass-balance model are reduced to: (1) correction factor for precipitation C_{prec} and (2) one melt parameter.

F_M and $r_{snow/firn}$ (Equation (1)) are assumed to be directly proportional to each other. With $r_{snow} = c_s F_M$ and $r_{firn} = c_f F_M$, we reformulate the degree-day factor:

$$DDF(I, c_{s/f}) = F_M(1 + c_{s/f}\, I)$$

using Equation (1). $DDF(I, c_{s/f})$ is a function of the potential radiation I and the condition of the glacier surface. F_M is constant in the course of the year and is used for tuning. The simulated snow water equivalent S determines whether the proportionality factor for snow c_s ($S > 0$) or for firn c_f ($S = 0$) is used. c_s and c_f are taken from studies using the same temperature-index model (e.g. Huss and others, 2007) and have values of $c_s = 0.035$ and $c_f = 0.050$ (both in W^{-1} m^2). They represent albedo variations due to different surface types.

Measured winter balance is used to obtain a first approximation of C_{prec}, and summer balance allows us to estimate F_M. The mass-balance model is calibrated in three separate steps for each individual year.

1. C_{prec} is tuned so that the observed snow water equivalent at the date of the winter survey is matched by the model.

2. The model is run between the exact dates of the two successive late summer surveys using C_{prec} calibrated in step 1. The melt factor F_M is varied so that calculated specific mass balance matches the net balance measurement.
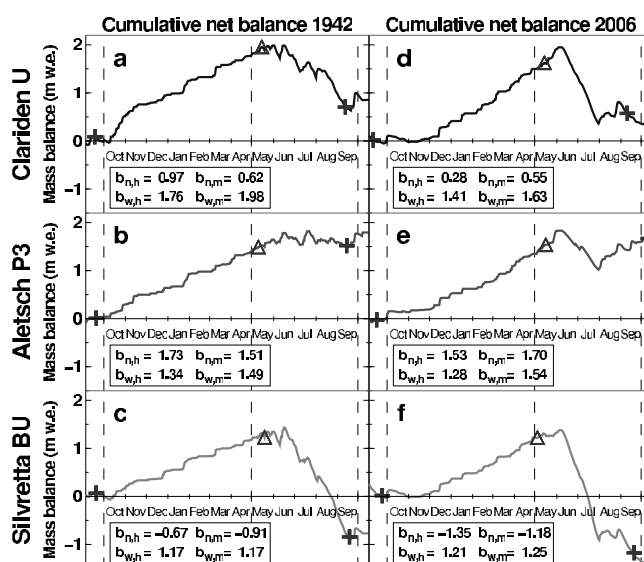

Fig. 3. Cumulative daily mass balance in two arbitrarily selected years: (a–c) 1942 and (d–f) 2006. Results of the stakes Clariden U, Aletsch P3 and Silvretta BU are shown. The winter balance measurement is indicated by a triangle, and net balance measurements by crosses. Dashed vertical lines refer to fixed-date time periods of homogenized mass balance. A comparison of homogenized ($b_{n,h}$, $b_{w,h}$) and measured mass-balance quantities ($b_{n,m}$, $b_{w,m}$) (m w.e.) is shown in the boxes.

3. As the accumulation period is rarely free of melt and the ablation period rarely free of solid precipitation, the previously determined parameters C_{prec} and F_M represent an initial guess, and need to be iteratively recalibrated in order to reproduce both the winter and net balance measurements within <0.05 m w.e.

An individual parameter set for each year with complete field data (b_w, b_n) is therefore obtained. During years with incomplete datasets (Fig. 2), mean values of C_{prec} and F_M for all complete years are used.

Examples for the calculated daily mass-balance time series during an annual cycle are presented in Figure 3. The calculated mass-balance curve matches the direct observations of winter and net balance and allows mass balance for arbitrary periods to be evaluated. Measured ($b_{n,m}$, $b_{w,m}$) and homogenized ($b_{n,h}$, $b_{w,h}$) mass-balance quantities may vary considerably as a result of the differences between the effective observation dates and fixed evaluation periods (see boxes in Fig. 3).

Trend analysis

In order to analyze trends in the mass-balance time series we apply the non-parametric Mann–Kendall (MK) test, which is widely used in hydrological applications for trend detection (e.g. Helsel and Hirsch, 1992). This rank-based procedure is especially suitable for non-normally distributed data and is robust against outliers and data gaps. The MK test yields a trend test statistic that allows the rejection of the null hypothesis at a certain significance level (Birsan and others, 2005). The slope of trends significant at the 99% level of the MK test is estimated using the Theil–Sen method, which is suitable for almost linear trends and is not affected by non-normal data and outliers (Helsel and Hirsch, 1992).
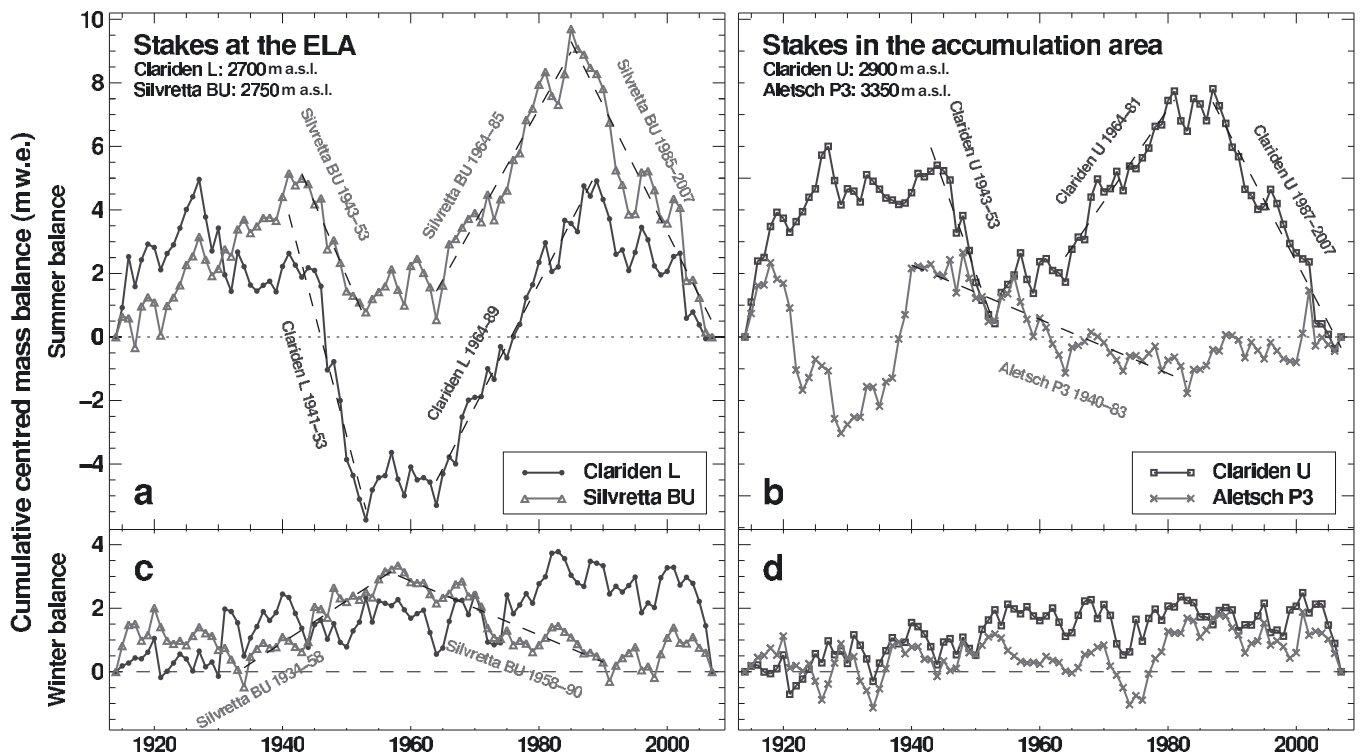
Fig. 4. Cumulative centred time series of summer and winter balance for (a, c) Clariden L and Silvretta BU and (b, d) Clariden U and Aletsch P3. The scales for summer and winter balance are the same. Dominant trends are indicated by dashed lines and corresponding text lines. For a complete trend analysis see Figure 5.

RESULTS

The mass-balance regimes at the four investigated sites show significant differences (Fig. 3). Although high winter accumulation is observed at Clariden U and L, Silvretta BU exhibits a drier climate (Table 2). Aletsch P3 is characterized by a regime with positive summer balances, whereas the stakes U, L and BU suffer net ablation in the summer season. Clariden L and Silvretta BU are located near the long-term equilibrium line; Clariden U and Aletsch P3 are in the accumulation area in all years (Table 2).

Direct comparison of point balances is complicated by the different mass-balance regimes. We subtract the 1914–2007 average of each time series from annual values (Table 2), obtaining time series of the deviation from the long-term average. This quantity is referred to as 'centred' mass balance. Positive (negative) centred mass balances are interpreted as above (below) the stake average of the considered quantity in the period 1914–2007. Centred mass balances allow the

analysis of mass-balance fluctuations, which are separated from the mass-balance regime at the study site.

Significant regional and altitudinal differences between the individual sites are evident in the cumulative centred balance curves (Fig. 4). At all stakes, the temporal variation in winter balance is much smaller than in summer balance. This is consistent with previous studies (Vincent and others, 2004; Huss and others, 2008a) and highlights the fact that glacier recession in the 20th century is mainly driven by increased melt in the summer months. Clariden L exhibits notably low centred summer balances in the 1940s, whereas the most important decrease at Silvretta BU has taken place since the mid-1980s (Fig. 4a). The stakes located below 3000 m a.s.l. (U, L, BU) show positive trends in the cumulative centred summer balances between the mid-1960s and the mid-1980s. For Aletsch P3, however, there is an opposite trend at the same time. This is not due to anomalously high winter balances at Aletsch P3, but reveals altitudinal differences in the reaction of summer balances to 20th-century climate warming on summer balances (Fig. 4). A similar observation in the western Alps is reported by Vincent and others (2007).

The cumulative centred time series of summer and winter balance (Fig. 4) were systematically analyzed in terms of prevailing trends. Trends over periods longer than 10 years were detected visually between break points in the time series. Between two and four long-term trends in both summer and winter balance, significant at the 99% level according to the MK test, could be identified for each site (Fig. 5). Negative trends in the cumulative centred summer balance occurred between 1943 and 1953 and between 1987 and 2007; positive trends are found between 1964 and 1985. However, Aletsch P3 exhibits completely different periods of dominant trends in summer and in winter (Fig. 4). The lengths of

Table 2. Measurement site characteristics: net balance $\overline{b_n}$, winter $\overline{b_w}$ and summer balance $\overline{b_s}$, total annual accumulation $\overline{c_a}$ and ablation $\overline{a_a}$ represent 1914–2007 averages in m w.e. a^{-1}

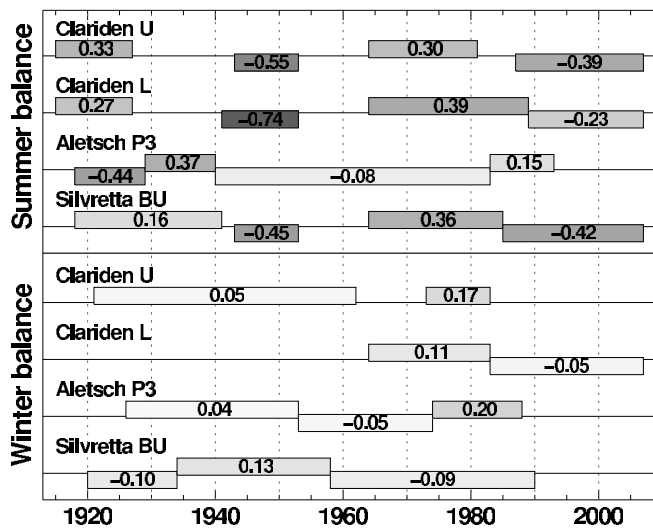| Stake	$\overline{b_n}$	$\overline{b_w}$	$\overline{b_s}$	$\overline{c_a}$	$\overline{a_a}$
U	1.31	2.00	−0.69	3.39	−2.08
L	0.32	1.93	−1.61	3.19	−2.87
P3	2.18	1.73	0.45	3.13	−0.95
BU	−0.10	1.37	−1.47	2.32	−2.42

Fig. 5. Dominant trends in cumulative centred summer and winter balance for the four stakes. Bars indicate the period and the sign of individual trends; numbers give the slope of the trend ($m w.e. a^{-1}$). 'Strong' trends (steep slope) have a darker shading.

Fig. 6. Mean centred summer and winter balances of the four stakes in seven 13 year periods.

the trends are similar for Silvretta BU, Clariden U and L, but are rarely the same. The trends in the cumulative centred winter balance generally have smaller slopes and are even less consistent than the summer balance trends (Fig. 5).

We divided the study period into seven sub-periods (I–VII) of 13 years (Fig. 6). This arbitrary subdivision of the dataset corresponds best to the periods of dominating trends (Fig. 5). Three sub-periods (II, IV, V) controlled by positive centred summer balances and three periods (III, VI, VII) with predominantly negative values are found. The sign of the centred summer balance at Aletsch P3, however, is opposite in sub-periods IV–VII (Fig. 6). The summer balance at high altitudes is significantly different from that of the long-term equilibrium line.

The anomalously low summer balances of Clariden L in period III may be related to a complete wastage of the firn coverage in the succession of warm years in the 1940s, which caused a positive feedback of surface albedo on the summer ablation rates and is responsible for the large difference compared to Clariden U (Fig. 6). Above-average winter accumulation probably reduced the impact of the same process at Silvretta BU.

Winter balances are below the long-term average in periods VI and VII (Fig. 6b). This is partly due to a prolongation of the melting season that successively extends into the period used for the determination of winter balance. Our model results indicate significant trends of about 2 days $(10 a)^{-1}$ towards a longer melting season for all stakes except Aletsch P3. The trends are even steeper for the final two decades. The increase in days with melt occurring at the equilibrium line is attributed to higher air temperatures in early summer and late fall and leads to a longer exposure time of low albedo surfaces with enhanced melt rates.

We evaluated the annual fraction of solid precipitation compared to total precipitation (Fig. 7a). This variable was chosen to further highlight the potential impact of temperature change on accumulation. On average, 79% of the annual precipitation occurs as snow at the stake sites. After a culmination around 1970, a significant decrease of the solid precipitation fraction is found. This implies that a consider-
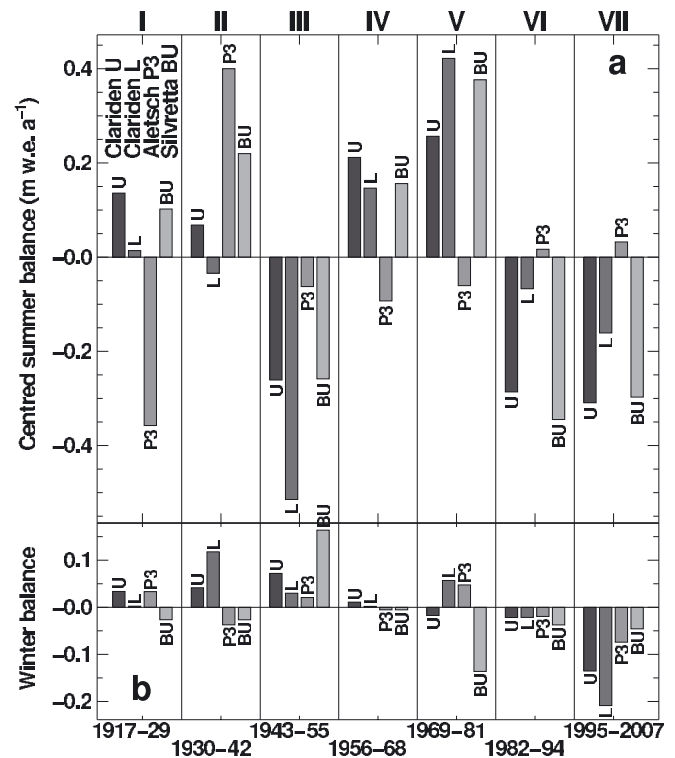
able amount of potential accumulation is lost at elevations at or above the equilibrium line, due to positive air temperatures during snowfall events (assuming no refreezing in the snowpack). This positive feedback effect (increasing temperature, decreasing solid precipitation fraction) has the potential to considerably accelerate glacier wastage.

The total annual ablation a_a at the site, calculated using field data and the model, is used to determine the corresponding energy consumed for melt E_m. We consider this quantity to be an excellent indicator for the climatic forcing on glaciers. a_a is converted into E_m ($W m^{-2}$) using the latent heat of fusion of $334 000 J kg^{-1}$. On average, between $10 W m^{-2}$ (P3) and $30 W m^{-2}$ (L) were consumed for snow- and ice-melt at the stake sites during the study period. There is an altitudinal gradient in climatic forcing of about $-3 W m^{-2} (100 m)^{-1}$ (Table 3). Our values of melt energy consumed are lower than those published by Vincent and others (2004) for the melting season on Glacier de Sarennes, western Alps. This is due to the fact that our study considers the total melt integrated over 1 year (1 October–30 September). This allows the evaluation of E_m time series, which are not biased by the varying length of the melting season.

The climatic forcing at Clariden U and L is very similar except for a shift due to different elevation (Fig. 7b). Throughout most of the 20th century, significantly less energy is consumed for melt at Silvretta BU than at Clariden L although the stake elevations only differ by 50 m. The mean degree-day factor is lower by 24% for Silvretta BU than for the other sites (Table 4). This cannot be explained by exposure alone. The lower climatic forcing at Silvretta BU inferred from the long-term point mass-balance measurements is consistent with the observation of reduced rates of glacier-wide mass loss of Silvrettagletscher compared to other Alpine glaciers (Bauder and others, 2007; Huss and others, 2008a).
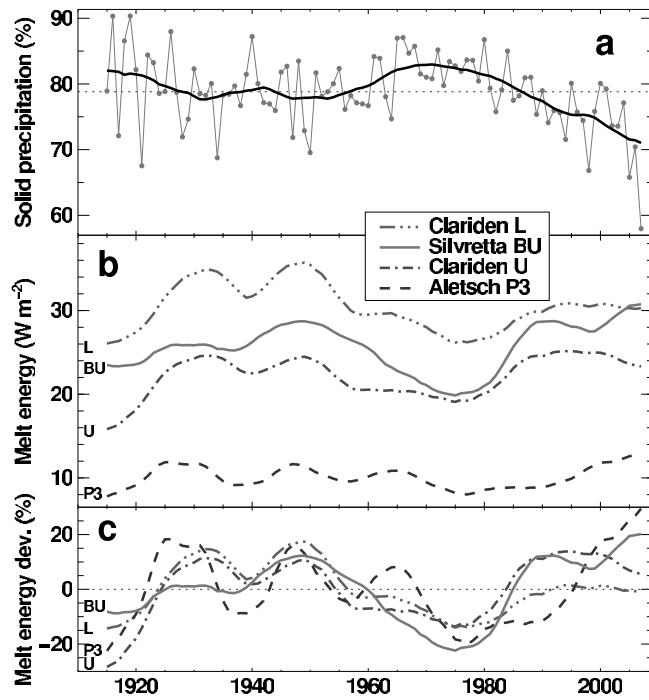
Fig. 7. (a) Four-stake average of the fraction of solid precipitation relative to total precipitation smoothed with a 10 year running mean (bold) (dotted line is 1914–2007 mean). (b,c) Ten-year running means of (b) energy consumed for melt at the four stakes and (c) the relative deviations from the 1914–2007 mean. Annual values are not shown for clarity.

The amount of energy consumed for melt significantly decreased during the 1960s to 1980s, causing the specific summer balance at three stakes to be above average (Figs 4 and 6). Strong regional differences in climatic forcing between Silvretta and Clariden are evident from Figure 7b. Although E_m at Silvretta BU was almost as low as at Clariden U, it meets the level of Clariden L at present. This shift in climatic forcing is interpreted as a result of regionally differing climate change conditions and has a magnitude of $6\,W\,m^{-2}$, corresponding to a shift in elevation of about 200 m.

We analyzed three periods with dominant trends in the cumulative centred summer balance (Fig. 5) and calculated the relative deviation of the period mean E_m from the 1914–2007 stake average (Table 3). The climatic forcing was significantly higher in the 1940s than during the period 1987–2007, except for Silvretta BU. During the period of positive

Table 3. Energy consumed for melt E_m at the four stakes: mean E_m in 1914–2007 and relative mean deviations from the 1914–2007 average for three periods

Stake	E_m	Deviation from 1914–2007 mean		
		1943–1953	1964–1985	1987–2007
	$W\,m^{-2}$	%	%	%
U	22.1	+14.0	−9.7	+12.2
L	30.4	+20.3	−10.3	+1.0
P3	10.0	+18.0	−10.9	+6.5
BU	25.1	+13.1	−21.0	+13.9

Table 4. Mean degree-day factor for snow $\overline{DDF_{snow}(\bar{I})}$ $(mm\,d^{-1}\,{}^\circ C^{-1})$ and mean precipitation correction factor $\overline{C_{prec}}$ (–) in 1914–2007, with standard deviations σ of annual parameter values

Stake	$\overline{DDF_{snow}(\bar{I})}$	σ_{DDF}	$\overline{C_{prec}}$	$\sigma_{C_{prec}}$
U	3.73	0.84	2.67	0.37
L	3.93	0.83	2.68	0.39
P3	3.97	0.99	3.10	0.64
BU	2.96	0.62	2.80	0.44

centred mass balances (1964–85) E_m was up to 20% below average. The time-series analysis at the four locations reveals similar fluctuations and relative offsets of E_m from the mean values (Table 3; Fig. 7c). This indicates that the trends in 20th-century climate forcing have extended to all four stake sites located at different elevations. However, there are substantial regional differences; the increase in climate forcing observed in the 1980s at three sites starts one decade later at Aletsch P3 and is much stronger at Silvretta BU compared to those on Claridenfirn (Fig. 7c).

DISCUSSION

Uncertainties in the homogenized seasonal time series of specific mass balance are due to several factors, which are either directly related to the measurements or to the homogenization procedure. Müller and Kappenberger (1991) identified the following biases in direct mass-balance measurements (numbers in brackets give the estimated error in m w.e.): (a) accumulation before and ablation after field visits in late summer ($\sigma_a = \pm0.2$), (b) melt-in of the stake ($\sigma_b = +0.1$), (c) compaction of firn layer ($\sigma_c = -0.1$), (d) determination of snow or firn density ($\sigma_d = \pm0.05$) and (e) percolation with refreezing mainly at the onset of the melting season ($\sigma_e = +0.05$). Most importantly, ablation after the field visits in late summer can be responsible for considerable differences in snow depth resulting from stake reading and snow probings. We address this bias using the daily mass-balance model. The other biases are difficult to detect and to correct and are assumed to be significant only in a few cases. The total uncertainty in the direct determination of mass balance is estimated to be ±0.25 m w.e. a^{-1}.

Years with no measurements available (Fig. 2) are completed using average model parameters calibrated for all years covered with data. Considering the significant year-to-year variability of DDF(I, $c_{s/f}$) ($\pm22\%$) and C_{prec} ($\pm16\%$, Table 4), the uncertainty in the reconstructed values may be substantial. However, our statistical model is considered to be the best way to address data gaps in order to obtain continuous time series.

In years with a complete set of field data (b_w, b_n), the potential for errors due to the mass-balance model is low, as it is well constrained by the seasonal data points. We suspect a tendency of the model to overestimate melt after the late summer field survey. The radiation conditions, often observed in autumn with high longwave outgoing radiation, are not properly accounted for in our model and may substantially reduce the melt rates (Ohmura, 2001). The potential for erroneous results, however, is low as moderate air

temperatures and reduced incoming radiation generally lead to relatively small amounts of melt in this season of the year.

Summer accumulation is insufficiently resolved by the seasonal mass-balance data because it is continuously melted away. The mass-balance model calculates summer accumulation, but could overestimate this term by compensating for it with increased melt rates. This would have an impact on the calculated total ablation and consequently on E_m.

With glacier retreat, a reduction in surface elevation at the stake location is inevitable. In order to shed light on the impact of this bias on specific mass balance, we analyzed the elevation changes using repeated DEMs. Glacier surface subsided by between 10 m (P3) and 21 m (L) since 1914. We calculated the change in E_m between the maximum and the minimum stake elevation. Surface lowering causes an additional forcing of the order of $+0.5\,W\,m^{-2}$, corresponding to $+0.05$ m w.e. or 2% of the mean annual melt.

The mass-balance observations used in this study are performed at fixed locations. The stakes are moved back to their original locations annually. This implies that (1) the exposure to solar radiation is constant, (2) the deposition or erosion of snow can be assumed to be similar in all years, and (3) the observed mass-balance quantities directly reflect the climatic forcing and are not biased by changing glacier surface area or uncertain spatial extrapolation of mass balance. This manifests an important advantage compared to glacier-wide average mass-balance quantities.

The evaluation of mass-balance quantities between fixed dates allows the comparison of different mass-balance time series on the basis of equal time periods. The choice of the fixed dates is debatable and has an impact on the evaluated values of winter and summer balance. The absolute maximum of snow cover often occurs in late May or June at the study sites (Fig. 3). We chose 30 April for the termination of the winter period because melt starts to be important around this date. When shifting the evaluation date to 31 May, our conclusions remain valid.

The two parameters of the mass-balance model are allowed to vary freely in order to obtain an exact match of the measurements. The year-to-year fluctuations in C_{prec} and DDF(I, $c_{s/f}$) do not, however, hamper the applicability of the mass-balance model because it is not regarded as a strictly physical model but as a statistical tool for scaling measured weather data to direct mass-balance observations. Moreover, the variation in C_{prec} and DDF(I, $c_{s/f}$) can be interpreted in terms of local climate at the glacier site. Fluctuations in C_{prec} correspond to varying differences in precipitation between the valley weather station and the stake site; C_{prec} is a measure for the altitudinal precipitation gradient and also captures anomalous snowdrift in individual years. DDF(I, $c_{s/f}$) is the proportionality factor between positive air temperatures and snow- or ice-melt. Year-to-year variations in DDF(I, $c_{s/f}$) can be due to the uncertain extrapolation of temperature from the valley station to the stake site. In addition, varying heat budget components, for example in terms of different air moisture or cloudiness (Pellicciotti and others, 2005), may influence the statistical relation between air temperature and melt rate.

We analyzed the calibrated annual values of $\overline{DDF_{snow}}(\bar{I})$ with $\bar{I}$ being the annual average of the potential direct radiation I. There is a constant level in $\overline{DDF_{snow}}(\bar{I})$ until 1960 when a decreasing trend begins (Fig. 8a). Compared to the beginning of the 20th century, more positive degree-days are currently required to melt the same quantity of snow. This is
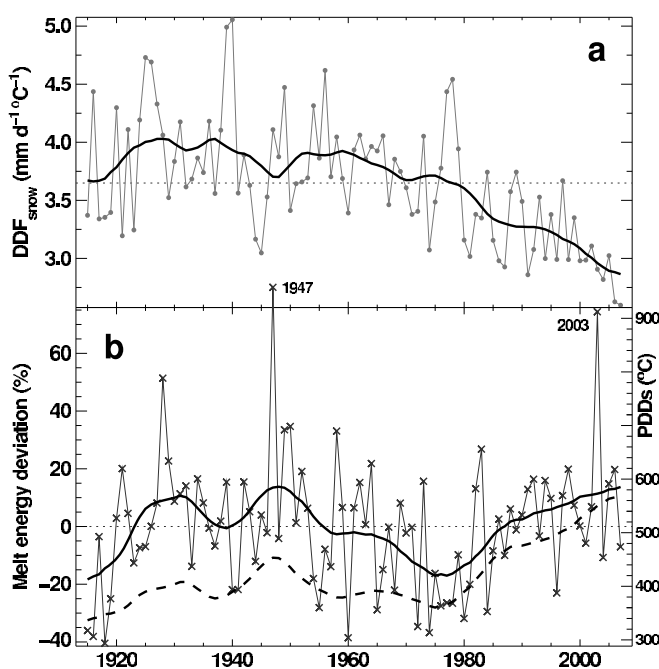

Fig. 8. Annual four-stake average of (a) the calibrated degree-day factor for snow $\overline{DDF_{snow}}(\bar{I})$ and (b) the four-stake average of the relative melt energy deviations from the mean (dashed) and the sum of positive degree-days (PDDs). Bold lines indicate 10 year running means.

intriguing, as decreasing surface albedo, reported for alpine glaciers (Paul and others, 2007), would have the opposite effect. A decrease in the temperature gradient between the weather station and the glacier site could explain the negative trend in the degree-day factors. This effect is not assumed to be very important, however, as temperatures used for the modelling were recorded at high-altitude stations with limited elevation differences to the glacier sites. We attribute the decreasing proportionality between positive air temperatures and the melt rate to a change in the relative importance of radiative fluxes at the study sites. Our present data do not allow us to shed light on the drivers of these changes in the heat budget, and further investigation is required.

The decadal fluctuations in melt energy consumed are consistent at all sites (Fig. 7c; Table 3) and were averaged over the four stakes (Fig. 8b). E_m culminates in the extreme year of 1947 that exhibits a higher climatic forcing than 2003 with its famous European heatwaves. We observe an increase in climatic forcing of 30% between 1975 and 2005. Ohmura and others (2007) attributed the higher melt rates observed since the 1980s to a global brightening of solar radiation and the enhanced greenhouse effect of terrestrial radiation.

The change in proportionality between the positive degree-days (PDDs) and the melt is evident from the comparison of these variables. At present, the annual sum of PDDs has increased to values unprecedented in the last century; however, the melt energy consumed shows no significant long-term trend (Fig. 8b). This discrepancy leads to a decrease in the calibrated degree-day factors. There is some anticorrelation between E_m and $\overline{DDF_{snow}}(\bar{I})$; the degree-day factor is low in periods of intensive climatic forcing and higher during years with less melt (Fig. 8b). The observation of decreasing degree-day factors with increasing climatic forcing could substantially hamper the applicability of temperature-index

models for projections of future glacier melt. It is important to understand the drivers of this changing proportionality between PDDs and melt in order to develop methods to tackle this problem.

CONCLUSIONS

Four long-term time series of seasonal mass-balance observations at fixed locations have been compiled. Each dataset was homogenized using a mass-balance model to account for the varying date of observations, correct for measuring bias, fill gaps and separate accumulation and ablation. A unique data basis has been assembled covering most of the 20th century. We find evidence for significantly different regional changes in the precipitation and melting conditions. A high-altitude site exhibits opposite trends in summer balance compared to the other series. Since 1975, the melt rates have increased by $10\% \, (10 \, a)^{-1}$. The analysis of the energy consumed for melt shows that the climatic forcing on Alpine glaciers was higher in the period 1943–53 than during the period 1987–2007. We find differing trends in climatic forcing and positive air temperatures since 1960. This observation is probably related to a change in the surface heat budget at the equilibrium line of glaciers, and has important implications for the long-term stability of empirical degree-day factors in temperature-index modelling over time.

The main goal of point mass-balance observations is to study variability and changes in climate at high-altitude sites. Our analysis shows the potential of long-term time series for inferring regional and altitudinal differences in climatic forcing. The homogenized 93 year time series of point-based seasonal mass balance at four different locations throughout the Alps are a unique dataset for investigating high-Alpine climatic changes throughout the 20th century. The continuation of long-term point mass-balance time series is therefore highly recommended for future mass-balance monitoring strategies.

ACKNOWLEDGEMENTS

REFERENCES

Aellen, M. 1996. Glacier mass balance studies in the Swiss Alps. *Z. Gletscherkd. Glazialgeol.*, **31**(1–2), 159–168.

Bauder, A., M. Funk and M. Huss. 2007. Ice-volume changes of selected glaciers in the Swiss Alps since the end of the 19th century. *Ann. Glaciol.*, **46**, 145–149.

Begert, M., T. Schlegel and W. Kirchhofer. 2005. Homogeneous temperature and precipitation series of Switzerland from 1864 to 2000. *Int. J. Climatol.*, **25**(1), 65–80.

Birsan, M.-V., P. Molnar, P. Burlando and M. Pfaundler. 2005. Streamflow trends in Switzerland. *J. Hydrol.*, **314**(1–4), 312–329.

Firnberichte 1914–78. Der Firnzuwachs 1913/14–1976/77 in einigen schweizerischen Firngebieten. *Vierteljahrsschr. Naturforsch. Ges. Zürich*, **1–64**.

Glaciological reports. 1916–2008. The Swiss Glaciers, 1913/14–2002/03. *Yearbooks of the Cryospheric Commission of the Swiss Academy of Sciences (SCNAT)*, **35–124**. Published since 1964 by VAW-ETHZ. Zürich.

Helsel, D.R. and R.M. Hirsch. 1992. *Statistical methods in water resources.* New York, Elsevier Science Publishers.

Hock, R. 1999. A distributed temperature-index ice- and snow-melt model including potential direct solar radiation. *J. Glaciol.*, **45**(149), 101–111.

Huss, M., A. Bauder, M. Werder, M. Funk and R. Hock. 2007. Glacier-dammed lake outburst events of Gornersee, Switzerland. *J. Glaciol.*, **53**(181), 189–200.

Huss, M., A. Bauder, M. Funk and R. Hock. 2008a. Determination of the seasonal mass balance of four Alpine glaciers since 1865. *J. Geophys. Res.*, **113**(F1), F01015. (10.1029/2007JF000803.)

Huss, M., A. Bauder and M. Funk. 2008b. Homogenization of long-term mass-balance time series. *Ann. Glaciol.*, **50** (see paper in this volume).

Kaser, G., J.G. Cogley, M.B. Dyurgerov, M.F. Meier and A. Ohmura. 2006. Mass balance of glaciers and ice caps: consensus estimates for 1961–2004. *Geophys. Res. Lett.*, **33**(19), L19501. (10.1029/2006GL027511.)

Lang, H., B. Schädler and G. Davidson. 1977. Hydroglaciological investigations on the Ewigschneefeld – Grosser Aletschgletscher: ablation, meltwater infiltration, water table in firn, heat balance. *Z. Gletscherkd. Glazialgeol.*, **12**(2), 109–124.

Meier, M.F. 1962. Proposed definitions for glacier mass budget terms. *J. Glaciol.*, **4**(33), 252–263.

Müller, H. and G. Kappenberger. 1991. Claridenfirn-Messungen 1914–1984. *Zürcher Geogr. Schr.* 40.

Müller-Lemans, H., M. Funk, M. Aellen and G. Kappenberger. 1995. Langjährige Massenbilanzreihen von Gletschern in der Schweiz. *Z. Gletscherkd. Glazialgeol.*, **30**, 141–160.

Ohmura, A. 2001. Physical basis for the temperature-based melt-index method. *J. Appl. Meteorol.*, **40**(4), 753–761.

Ohmura, A., A. Bauder, H. Müller and G. Kappenberger. 2007. Long-term change of mass balance and the role of radiation. *Ann. Glaciol.*, **46**, 367–374.

Paul, F., A. Kääb and W. Haeberli. 2007. Recent glacier changes in the Alps observed from satellite: consequences for future monitoring strategies. *Global Planet. Change*, **56**(1–2), 111–122.

Pellicciotti, F., B.W. Brock, U. Strasser, P. Burlando, M. Funk and J.G. Corripio. 2005. An enhanced temperature-index glacier melt model including shortwave radiation balance: development and testing for Haut Glacier d'Arolla, Switzerland. *J. Glaciol.*, **51**(175), 573–587.

Vincent, C., G. Kappenberger, F. Valla, A. Bauder, M. Funk and E. Le Meur. 2004. Ice ablation as evidence of climate change in the Alps over the 20th century. *J. Geophys. Res.*, **109**(D10), D10104. (10.1029/2003JD003857.)

Vincent, C., E. Le Meur, D. Six, M. Funk, M. Hoelzle and S. Preunkert. 2007. Very high-elevation Mont Blanc glaciated areas not affected by the 20th century climate change. *J. Geophys. Res.*, **112**(D9), D09120. (10.1029/2006JD007407.)